New insight into N_2 adsorption and ion-exchange features of CuMFI with different Si/Al ratios†

Atsushi Itadani,[a] Masashi Tanaka,[ab] Yasushige Kuroda*[b] and Mahiko Nagao[ab]

Received (in Durham, UK) 14th March 2007, Accepted 6th June 2007
First published as an Advance Article on the web 25th June 2007
DOI: 10.1039/b703846a

The effects of the Si/Al ratio of the mother MFI on the N_2 adsorption phenomena at 301 K and on the ion-exchange features of copper-ion-exchanged MFI zeolites (CuMFI) were investigated. The CuMFI samples were prepared by ion exchange in an aqueous solution of $Cu(C_2H_5COO)_2$, $Cu(CH_3COO)_2$, $CuCl_2$ or $Cu(NO_3)_2$. The sample with an Si/Al ratio of 19.8, which had been prepared by using a $Cu(C_2H_5COO)_2$ solution, exhibited extremely efficient N_2 adsorption in terms of both the number of adsorbed molecules and its energetic behaviour, as compared to samples with other Si/Al ratios and/or with other ion-exchange solutions. The coordination environment of the copper ion adsorbing N_2 on this sample was clarified for the first time by analysis of the EXAFS spectra. The IR and DR-UV-Vis spectra revealed that the state of exchanged Cu^{2+} in CuMFI differs remarkably, depending on the value of the Si/Al ratio of the MFI and the types of counter ion in the exchange solution. The Cu^{2+} species coordinated with propionate or acetate ion were preferentially ion-exchanged in samples with higher Si/Al ratios (*i.e.*, 19.8 and above), in comparison with aqua complexes of Cu^{2+} ions. From the measurements of heats-of-adsorption of CO and photoemission spectra, it was elucidated that the relative proportion of the number of the sites located in the neighbourhood of the three lattice oxygen atoms (*i.e.*, three-coordinate sites) to the total number of exchangeable sites in MFI including the two-coordinate sites increased with an increase in the Si/Al ratio; Cu^{2+} with propionate or acetate ion were exchanged selectively on the three-coordinate sites. The DR-UV-Vis and EPR spectroscopic signatures of two different Cu^{2+} species located in the two- and the three-coordinate sites were determined.

Introduction

Copper-ion-exchanged MFI zeolite (CuMFI), especially, non-stoichiometrically ion-exchanged sample (*i.e.*, ion-exchange level >100%), exhibits high levels of catalytic activity for the direct decomposition of NO into N_2 and O_2 species.[1,2] Furthermore, this material strongly adsorbs N_2 molecules, even at room temperature (r.t.).[3–5] A great deal of effort has thus far been expended in the analysis of the state of active sites on CuMFI that are effective with respect to NO decomposition or N_2 adsorption. It was previously shown that the monovalent copper ions (Cu^+) formed by heat treatment *in vacuo* act as active species.[1,3–5] Spectroscopic, calorimetric and theoretical data suggest the presence of two types of exchangeable site for copper ions in MFI;[3,6–10] our group has emphasized that two types of site are necessary for NO decomposition, whereas for N_2 adsorption, only one type is dominantly operated.[11–13] Recently, it was also demonstrated that the N_2-adsorption properties of CuMFI differ depending on the types of counter ion in the exchange solution employed.[14–17]

The molar ratio of SiO_2 to Al_2O_3 (*i.e.*, the Si/Al ratio), which comprise a zeolite matrix, is among the factors that govern the unique properties of zeolite (*e.g.*, ion-exchange features, catalytic activity, gas-adsorption properties, *etc.*).[18] Many studies have been reported regarding the effects of the Si/Al ratio of the mother zeolite on NO-decomposition activity.[19] However, the effects of the Si/Al ratio on the N_2-adsorption properties, as well as the effects on the state of exchanged copper ions, have not yet been clarified.

In the present study, we examined the effect of the Si/Al ratio on the N_2-adsorption properties at 301 K of CuMFI. Moreover, the effects of the Si/Al ratio on the state of exchanged copper ions in CuMFI and on the reduction properties of copper ions *via* heat treatment *in vacuo* were also elucidated.

Results and discussion

The adsorption isotherms of N_2 at 301 K for the 873 K-treated CuMFI(P) samples are shown in Fig. 1. The notation of the samples is described in the Experimental section and ESI.† For all samples, a remarkable increase in the adsorbed amounts is seen in the lower pressure region, which indicates a strong interaction between the Cu^+ ions formed in CuMFI and the N_2 molecules. Moreover, the adsorption amount of N_2 reaches

[a] *Research Laboratory for Surface Science, Faculty of Science, Okayama University, Tsushima-naka, Okayama, 700-8530, Japan*
[b] *Department of Fundamental Material Science, Graduate School of Natural Science and Technology, Okayama University, Tsushima-naka, Okayama, 700-8530, Japan. E-mail: kuroda@cc.okayama-u.ac.jp; Fax: +81 86-251-7853; Tel: +81 86-251-7844*

† Electronic supplementary information (ESI) available: Details of samples preparation, heats-of-adsorption of N_2 for CuMFI(P)-19.8-109 and EPR spectra of CuMFI(C)-35.0-132 and CuMFI(N)-100-73. See DOI: 10.1039/b703846a

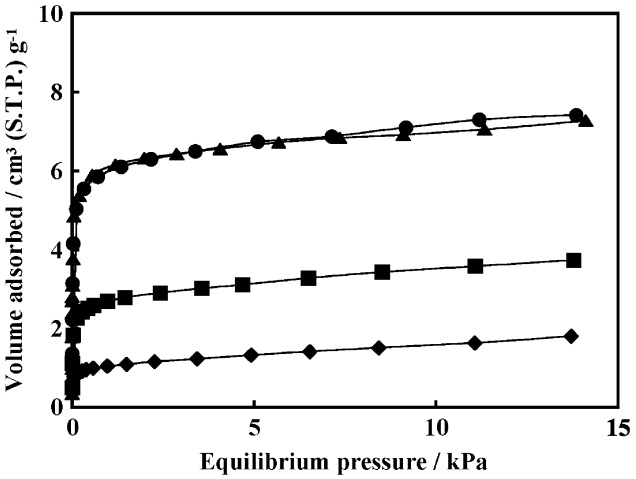

Fig. 1 Adsorption isotherms of N_2 at 301 K for CuMFI(P): (●) CuMFI(P)-11.9-109, (▲) CuMFI(P)-19.8-109, (■) CuMFI(P)-35.0-105 and (◆) CuMFI(P)-100–102.

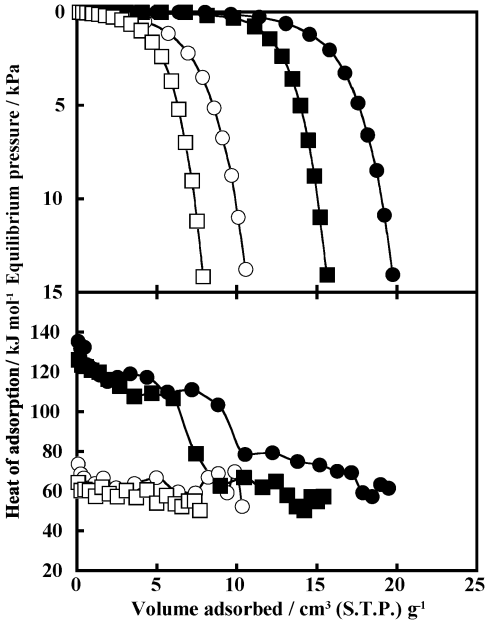

Fig. 2 Adsorption isotherms and differential heats of adsorption of CO at 301 K: (●,○) CuMFI(P)-11.9-109 and (■,□) CuMFI(P)-19.8-109. Filled and open symbols represent the first and second adsorption, respectively.

a saturated value with an increase in the equilibrium pressure of N_2 (*i.e.*, a Langmuir-type isotherm). The distinct difference in the adsorbed amounts among samples was due to differences in the Si/Al ratios, that is, the absolute number of exchangeable sites for copper ions in the MFI was different in each case. To obtain accurate information regarding N_2 adsorption on CuMFI, we estimated the number of adsorbed N_2 molecules per copper ion, $n_{N_2}/N_{Cu(total)}$ (Table 1). The results obtained for CuMFI(A) and CuMFI(C) are also listed in this table. Here, we need not elaborate on the results for CuMFI(N); in the case of the ion-exchange method used, non-stoichiometrically ion-exchanged sample could not be prepared.[20] It is apparent that the value of $n_{N_2}/N_{Cu(total)}$ for CuMFI(P)-19.8-109 is the largest among the values obtained for CuMFI(P) with different Si/Al ratios. In addition, for CuMFI(P)-35.0-105 and CuMFI(P)-100-102, the $n_{N_2}/N_{Cu(total)}$ values are larger than that for CuMFI(P)-11.9-109. CuMFI(A) and CuMFI(C) samples also show the similar tendencies as CuMFI(P). Effective sites for N_2 adsorption were thus formed at a higher rate in the samples with Si/Al ratios of 19.8 and above.

The CO molecule is known to be useful as a probe molecule for the estimation of the number and the state of Cu^+ ions in zeolites, due to its preferential adsorption on Cu^+.[21–25] Fig. 2 presents the adsorption isotherms and the differential heats of adsorption of CO at 301 K for CuMFI(P)-11.9-109 and CuMFI(P)-19.8-109. The first adsorption measurement was performed at 301 K for the 873 K-treated sample, and after re-evacuation of the sample at 301 K for 4 h, the second adsorption measurement was carried out at the same temperature as that used for the first adsorption measurement. From these data, the ratio of the number of Cu^+ ions to the total number of copper ions in CuMFI, $N_{Cu^+}/N_{Cu(total)}$, was

Table 1 Analysis of adsorption data

	N_2 adsorption/cm^3 g^{-1}		CO adsorption/cm^3 g^{-1}				
	$V_{m(N_2)}$[a]	n_{N_2}[b]/$N_{Cu(total)}$[c]	$V_{m1(CO)}$[d]	$V_{m2(CO)}$[e]	$V_{chem(CO)}$[f]	N_{Cu^+}[g]/$N_{Cu(total)}$	n_{N_2}/N_{Cu^+}
CuMFI(P)-11.9-109	7.32	0.51	19.10	11.16	7.94	0.55	0.93
CuMFI(P)-19.8-109	7.13	0.83	14.80	8.05	6.75	0.78	1.06
CuMFI(P)-35.0-105	3.66	0.73	9.30	5.38	3.92	0.78	0.94
CuMFI(P)-100-102	1.23	0.68	3.73	2.38	1.35	0.75	0.91
CuMFI(A)-11.9-105	6.30	0.46	17.73	10.69	7.04	0.50	0.92
CuMFI(A)-19.8-100	6.15	0.78	13.27	7.35	5.92	0.75	1.04
CuMFI(A)-35.0-103	3.50	0.69	8.97	5.22	3.75	0.74	0.93
CuMFI(A)-100-101	1.07	0.57	3.63	2.50	1.13	0.60	0.95
CuMFI(C)-11.9-107	5.16	0.37	17.18	10.17	7.01	0.50	0.74
CuMFI(C)-19.8-113	6.01	0.71	13.06	6.98	6.08	0.72	0.99
CuMFI(C)-35.0-132	3.70	0.60	9.47	5.26	4.21	0.69	0.87
CuMFI(C)-100-125	1.02	0.47	3.56	2.40	1.16	0.53	0.88

[a] Monolayer capacity for adsorbed N_2 (at STP). [b] The number of adsorbed N_2 molecules based on $V_{m(N_2)}$ value. [c] The number of total copper ions obtained by titration. [d] Monolayer capacity obtained from the first adsorption isotherm of CO (at STP). [e] Monolayer capacity obtained from the second adsorption isotherm of CO (at STP). [f] Chemisorbed amount ($= V_{m1(CO)} - V_{m2(CO)}$). [g] The number of monovalent copper ions obtained from CO adsorption.

evaluated by the same method as that used in previous studies.[3] Here, the chemisorbed amount of CO and the content of copper-ion in the sample were used for the evaluation. The adsorption data and the values of $N_{Cu^+}/N_{Cu(total)}$ for these samples are listed in Table 1, together with those obtained for other samples. The ratio, $N_{Cu^+}/N_{Cu(total)}$, is larger for those samples with Si/Al ratios of 19.8 and above than it is in the case of the sample with an Si/Al ratio of 11.9. Thus, in the case of CuMFI samples with higher Si/Al ratios, the reduction of divalent copper ions to monovalent copper ions occurred readily, as compared to that in the sample with an Si/Al ratio of 11.9. In addition, when the extent of reduction is compared among samples with the same Si/Al ratio, it is quite obvious that the copper ions in samples prepared by using an aqueous solution of $Cu(C_2H_5COO)_2$ are easy to be reduced to the monovalent species. On the basis of the $n_{N_2}/N_{Cu(total)}$ and $N_{Cu^+}/N_{Cu(total)}$ values, we evaluated the ratio of the number of adsorbed N_2 molecules to the number of Cu^+ ions, n_{N_2}/N_{Cu^+} (Table 1). In general, to obtain high levels of catalytic activity and its reproducibility, the use of an aqueous solution of $Cu(CH_3COO)_2$ has known to be useful for the preparation of copper-ion-exchanged zeolites. The samples prepared by using a $Cu(C_2H_5COO)_2$ solution have higher adsorption capabilities for N_2 and CO, compared with the samples prepared by using a solution of $Cu(CH_3COO)_2$. It is thus important from the viewpoint of the development of a new preparation method of effective catalysts to elucidate the specificity of CuMFI(P). In this paper, we mainly characterized the active sites in CuMFI(P) with various Si/Al ratios and clarified the differences and the similarities between these CuMFI(P) samples and other samples. The state of Cu^+ ions formed in CuMFI was investigated by taking account of the adsorption-heat curves. For the first adsorption of both samples, the heats-of-adsorption of CO are 130–120 kJ mol^{-1} at the initial adsorption stage (chemisorption region), and these heats decrease in a stepwise manner to about 110 kJ mol^{-1} with increases in the adsorbed amounts, and then values of 55–50 kJ mol^{-1} are reached upon the completion of the monolayer. The heat curves obtained for the second adsorption are similar to those obtained for the latter half of the first adsorption, thus indicating that reversible adsorption takes place in the second adsorption. In the chemisorption region, which corresponds to adsorbed amounts of up to *ca.* 8 and 6 $cm^3\ g^{-1}$ for CuMFI(P)-11.9-109 and CuMFI(P)-19.8-109, respectively, we confirmed the existence of two types of Cu^+ species having different interaction energies with CO molecules: 120 and 110 kJ mol^{-1}. This is supported from the theoretical results.[26,27] Here, it is noteworthy that the Cu^+ ions, which give a CO adsorption-heat of 110 kJ mol^{-1}, are formed at a higher rate in CuMFI(P)-19.8-109 than in CuMFI(P)-11.9-109.

The photoemission spectra of the 873 K-treated samples are shown in Fig. 3. All of the photoemission bands are caused by the electronic transition from the $3d^94s^1$ to $3d^{10}$ levels of the Cu^+ ions formed in CuMFI.[7] By applying a curve-fitting technique to the observed bands, we resolved the bands into three components, that is, the bands centred at 21 000, 19 500 and 18 500 cm^{-1}. Thus far, the bands at 21 000 and 18 500 cm^{-1} have been attributed to emissions of Cu^+ existing on two

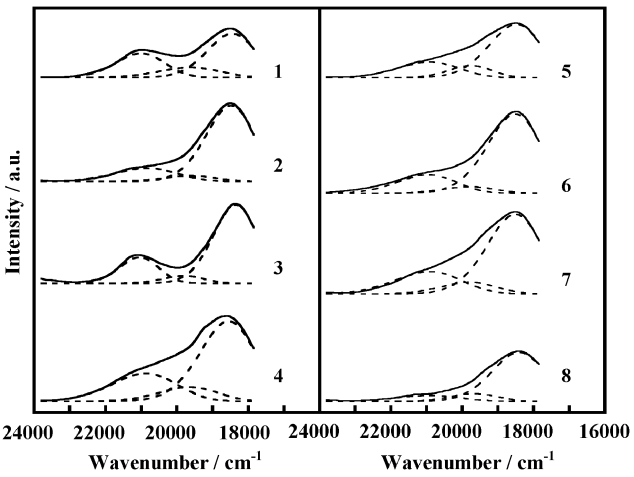

Fig. 3 Photoemission spectra of CuMFI: (1) CuMFI(P)-11.9-109, (2) CuMFI(P)-19.8-109, (3) CuMFI(A)-19.8-100, (4) CuMFI(C)-19.8-113, (5) CuMFI(P)-35.0-105, (6) CuMFI(A)-35.0-103, (7) CuMFI(C)-35.0-132 and (8) CuMFI(P)-100-102.

kinds of ion-exchangeable sites in MFI, where the respective species have two- and three-coordinate structures involving lattice oxygen atoms.[3,28] A weak 19 500 cm^{-1}-band is due to the emission of Cu^+ ions on the siliceous part of MFI.[3,28] In the case of CuMFI(P), strong emission bands for the sample with an Si/Al ratio of 11.9 are observed at 21 000 and 18 500 cm^{-1}, whereas for samples with an Si/Al ratio above 19.8, a band centred at 18 500 cm^{-1} is observed. It was thus found that the ion-exchange sites located in the neighbourhood of the three lattice oxygen atoms are present at a higher rate in MFI with higher Si/Al ratios. When the results shown in Fig. 2 are taken into account, two types of Cu^+ species giving CO adsorption-heats of 120 and 110 kJ mol^{-1} correspond to species responsible for photoemission bands at 21 000 and 18 500 cm^{-1}, respectively. In contrast to CuMFI(P)-19.8-109, in CuMFI(C)-19.8-113, the intense bands are also observed at around 21 000 and 19 500 cm^{-1}, in addition to the band centred at 18 500 cm^{-1}. The spectral feature of CuMFI(A)-19.8-100 is similar to that of CuMFI(P)-19.8-109 rather than to that of CuMFI(C)-19.8-113. From the photoemission spectra of CuMFI with the Si/Al ratios of 35.0 and 100, we could not distinguish the specificity of the sites occupied by copper ions among samples prepared by using different ion-exchange solutions; the site-occupancy of copper ions is remarkably different in the samples with an Si/Al ratio of 19.8.

The XANES and EXAFS spectra for CuMFI(P)-19.8-109 under various conditions are represented in Fig. 4. The observed XANES bands at 8.983 and 8.993 keV after evacuation of the sample at 873 K are representative bands assigned to the $1s–4p_\pi$ and $1s–4p_\sigma$ transitions of the Cu^+ ions, respectively.[29] The appearance of two such characteristic bands is explained that the Cu^+ ions assume a linear (two) or a planar (three) coordinate structure.[29,30] The band at 8.983 keV is markedly reduced in terms of intensity when the sample is exposed to N_2 gas at r.t., and the intensity of the band is recovered by re-evacuation of the sample at the temperature of exposure. Such changes in the intensity of the observed band have been interpreted as adsorption of N_2 molecules by the

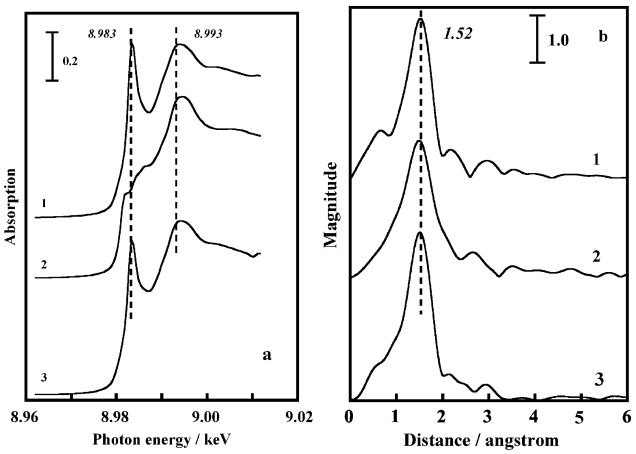

Fig. 4 (a) XANES and (b) EXAFS spectra for CuMFI(P)-19.8-109 under various conditions: (1) after evacuation at 873 K, (2) followed by exposure to N_2 gas at about 13 kPa and (3) re-evacuation at r.t.

three-coordinated Cu^+ species, thus rendering a pseudo-tetrahedral arrangement, and resulting in a decrease in the intensity of the 8.983 keV-band. In addition, changes in the intensity of the XANES bands are indicative of a strong interaction between the Cu^+ ions and N_2 molecules; this finding is also supported by the observation of a high heat value, 87 kJ mol^{-1}, for N_2 adsorption (ESI†). In the EXAFS spectra, a band due to back-scattering from the nearest neighbouring oxygen atoms is observed at 1.52 Å (no phase-shift correction) for the 873 K-treated sample. The parameters, which were obtained by analysis of the EXAFS data using the least-square method and by using Cu_2O as a reference substance, are as follows: N (Cu–O coordination number) = 2.7 ± 0.2, r (Cu–O distance) = 1.98 ± 0.01 Å and σ^2 (Debye–Waller factor) = 0.010 $Å^2$. Here, we were also able to confirm from these values that the copper ion in CuMFI(P)-19.8-109 is situated at the site with a three-coordinate environment. When the sample is exposed to N_2 gas, the band at around 1.5 Å increases in width and its intensity decreases, in comparison with the properties of the band obtained for the 873 K-treated sample. By re-evacuating the sample at r.t., this band recovered its original pattern. Thus, the changes observed in the EXAFS spectra also indicate a strong interaction between the copper ions and N_2 molecules. Analysis of the EXAFS data for the band at around 1.5 Å (using Cu_2O and $[Cu(NH_3)_2]^+$ as reference substances) gave the following parameters: N (Cu–O) = 2.7 ± 0.2, N (Cu–N) = 1.1 ± 0.1; r (Cu–O) = 1.97 ± 0.01 Å, r (Cu–N) = 1.91 ± 0.01 Å; σ^2 (Cu–O) = 0.013 $Å^2$, σ^2 (Cu–N) = 0.005 $Å^2$. These results are unambiguous evidence in support of the hypothesis that three-coordinated Cu^+ species are the active sites for specific N_2-adsorption at r.t. Furthermore, the EXAFS spectra values showed good agreement with the values obtained from the adsorption data (Table 1: $n_{N_2}/N_{Cu^+} = \approx 1$).

The effect of the Si/Al ratio on the state of exchanged copper ions in CuMFI was examined. The IR spectra for CuMFI(P)-11.9-68, CuMFI(P)-35.0-50 and NaMFI evacuated at r.t. are shown in Fig. 5. The intensity of the spectra was normalized, as described later (Experimental section). For each sample, two strong bands appear at approximately

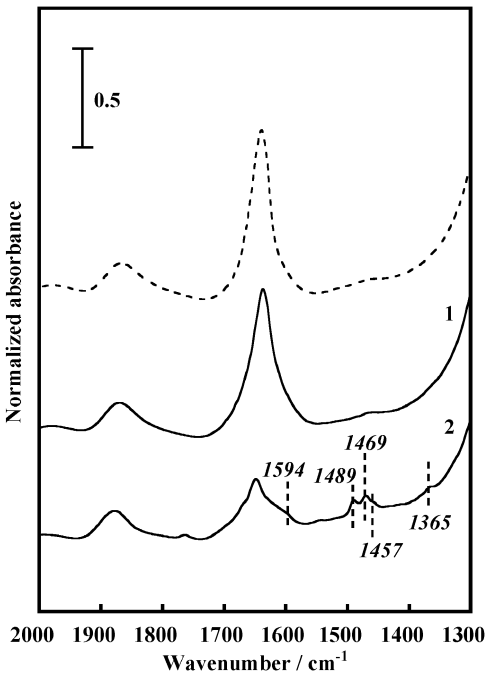

Fig. 5 IR spectra of CuMFI(P) and NaMFI in the wavenumber region of 2000 and 1300 cm^{-1}: (--) NaMFI, (1) CuMFI(P)-11.9-68 and (2) CuMFI(P)-35.0-50.

1860 and 1650 cm^{-1}, which indicates that these bands are derived from the mother MFI. In a study of HMFI (Si/Al = 14) treated at a high temperature, Zecchina and co-workers assigned such bands to a skeletal Si–O–Al mode.[31] In the present case, the 1650 cm^{-1}-band appears to involve another component band assignable to an H–O–H bending vibration of the water molecules physisorbed in the nanopores of MFI.[32] It is noteworthy that for CuMFI(P)-35.0-50, the characteristic bands appear at 1700–1300 cm^{-1}. These bands were also observed for CuMFI(P)-19.8-72 and CuMFI(P)-100-75. Moreover, similar bands appeared for CuMFI(A) with the Si/Al ratios of 19.8 and above. The respective bands observed at 1670, 1594, 1403 and 1308 cm^{-1} are assigned to the $–COO^-$ species in the propionate ion coordinated to Cu^{2+}, and the 1489, 1469, 1365 and 1340 cm^{-1}-bands are attributed to the CH_3 bending mode.[33] In the higher wavenumber region (not shown here), the C–H stretching vibration band due to the propionate ion also appeared clearly for CuMFI(P) with higher Si/Al ratios. As a matter of course, no such bands were observed for CuMFI(C) and CuMFI(N) with various Si/Al ratios. These results demonstrated that Cu^{2+} ions take the form of a complex with the propionate ion in CuMFI(P) with higher Si/Al ratios ($[CuC_2H_5COO]^+$). Taking into account the results shown in Fig. 2 and Fig. 3 it can be concluded that $[CuC_2H_5COO]^+$ were exchanged at three-coordinate sites.

Fig. 6 represents the DR-UV-Vis spectra of the samples evacuated at r.t. A broad band, which is assigned to a spin-allowed transition from ^2E_g to $^2T_{2g}$ of the Cu^{2+} ions in CuMFI,[34–37] appears for every sample. Judging from the absorption position of the observed band, the exchanged Cu^{2+} ions were considered to form the complexes coordinated with the oxygen atoms (in H_2O molecules, $C_2H_5COO^-$ ion or

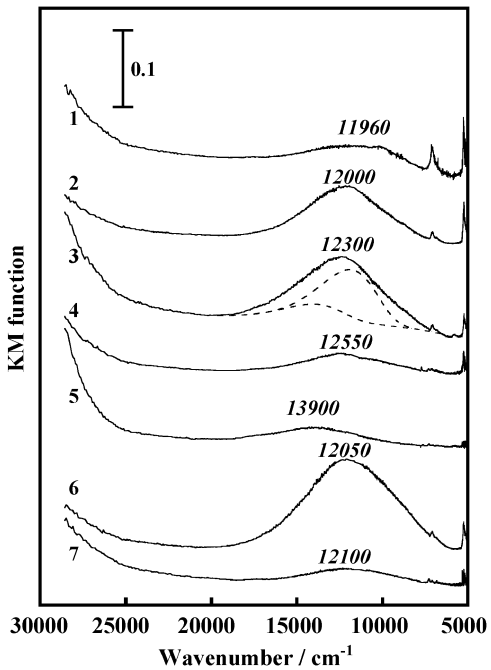

Fig. 6 DR-UV-Vis spectra of CuMFI: (1) CuMFI(P)-11.9-12, (2) CuMFI(P)-11.9-68, (3) CuMFI(P)-19.8-72, (4) CuMFI(P)-35.0-50, (5) CuMFI(P)-100-75, (6) CuMFI(C)-11.9-74 and (7) CuMFI(C)-100-90.

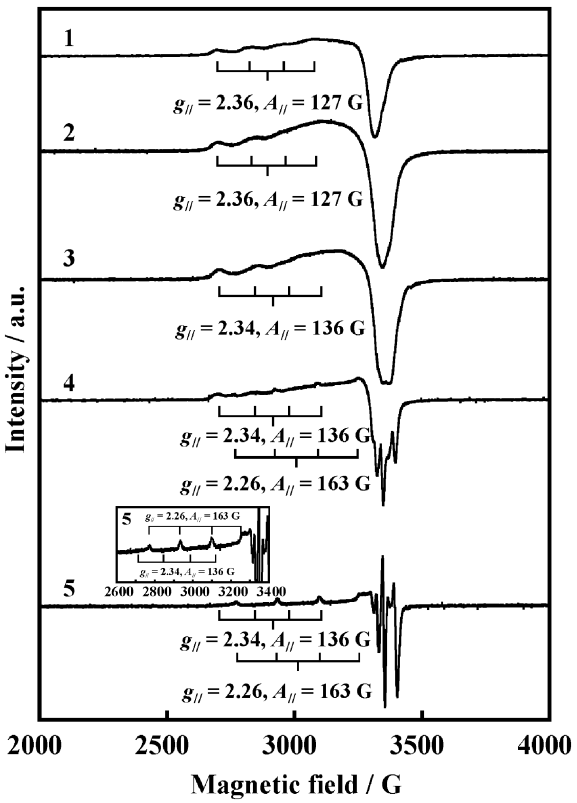

Fig. 7 EPR spectra of CuMFI(P): (1) CuMFI(P)-11.9-12, (2) CuMFI(P)-11.9-68, (3) CuMFI(P)-19.8-72, (4) CuMFI(P)-35.0-50, (5) CuMFI(P)-100-75.

OH^- ion) as a ligand. The position of the absorption maximum of the observed band for CuMFI(P)-11.9-12 is found to be almost the same as that for CuMFI(P)-11.9-68. It is important to note that for CuMFI(P), the absorption maximum of the band is observed at the side with the higher wavenumber with increasing Si/Al ratio of the sample. Similar tendency was also seen in CuMFI(A). By taking into consideration that the content of copper ions in CuMFI(P)-11.9-12 is equal to that in CuMFI(P)-100-75 (*i.e.*, the absolute amount), the coordination environment of Cu^{2+} ions in CuMFI(P) appears to differ, depending on the Si/Al ratio. In addition, for the samples with the Si/Al ratios of 35.0 and 100, a weak shoulder band is also seen at around 16 500 cm^{-1}. Here, we intended to resolve the observed band for CuMFI(P)-19.8-72 into the bands centred at 16 500, 13 900 and 12 000 cm^{-1}. The positions of these bands were referred to those of the bands for CuMFI(P)-100-75 (16 500 and 13 900 cm^{-1}) and CuMFI(P)-11.9-68 (12 000 cm^{-1}). The difference in the position of the maximum absorption of the observed band has been interpreted as a difference in the strength of the ligand field associated with Cu^{2+} ions in the samples after the ion-exchange operations. For CuMFI(C), the positions of the absorption maxima of the observed bands are almost the same (*ca.* 12 000 cm^{-1}), independent of the Si/Al ratio, indicating clearly that the states of Cu^{2+} ions in these CuMFI(C) samples differ from those in CuMFI(P) with higher Si/Al ratios.

The EPR spectra of the r.t.-treated CuMFI(P) samples are shown in Fig. 7. All of the spectra are due to the Cu^{2+} ions exchanged in the MFI.[36–42] In the case of both CuMFI(P)-11.9-12 and CuMFI(P)-11.9-68, a band derived from the Cu^{2+} ions with axial anisotropy is observed at about 3400 G, thus indicating that the rotation of electron spin in Cu^{2+} ions are restricted. In CuMFI(P) samples with Si/Al ratios of 19.8 and above, a sharp and well-resolved band is clearly seen in a magnetic field that is similar to the bands observed for samples with an Si/Al ratio of 11.9; analogous spectra were observed for CuMFI(A). Interestingly, bands similar to those for CuMFI(P) with the Si/Al ratios of 11.9 and 19.8 were observed in the case of the r.t.-treated CuMFI(C) and CuMFI(N) samples (Si/Al ratios of 35.0 and 100; ESI†). The characteristic bands observed for CuMFI(P) with higher Si/Al ratios can be interpreted as follows; the higher the Si/Al ratio of MFI, the lower the absolute number of copper ions contained in sample, and thus the probability of spin–spin coupling between copper ions decreases, resulting in the EPR band being sharp. Furthermore, special attention was paid to the band on the side with the low magnetic field. As regards CuMFI(P)-35.0-50 and CuMFI(P)-100-75, we were able to discriminate between two types of Cu^{2+} species that differed in terms of coordination structure by two parameters, $g_{\|} = 2.34$, $A_{\|} = 136$ G and $g_{\|} = 2.26$, $A_{\|} = 163$ G. The Cu^{2+} ions that give the $g_{\|}$ values of 2.34 and 2.26 in CuMFI(P)-35.0-50 and CuMFI(P)-100-75 are subjected to a stronger ligand field, as compared to species in other CuMFI(P)-11.9 samples with the $g_{\|}$ value of 2.36. This finding is in good agreement with the results deduced from the DR-UV-Vis spectra (Fig. 6). It appears that in CuMFI(P), Cu^{2+} ions that yield the parameter $g_{\|} = 2.36$, 2.34 and 2.26 correspond to the species showing the DR-UV-Vis band centred at 12 000, 13 900 and 16 500 cm^{-1}, respectively. Taking account of the results of IR spectra, the Cu^{2+} ions giving the

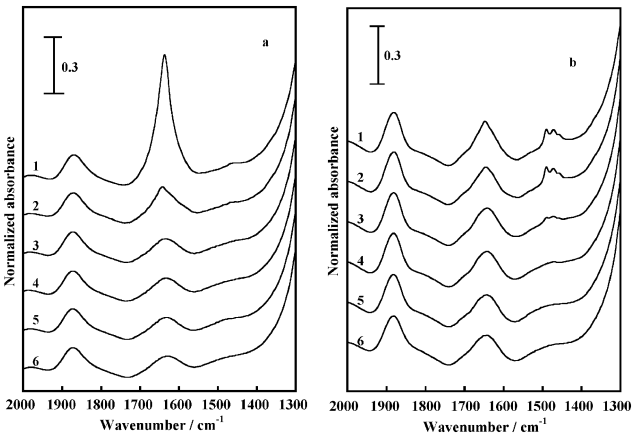

Fig. 8 IR spectra of (a) CuMFI(P)-11.9-68 and (b) CuMFI(P)-100-75 in the wavenumber region of 2000 to 1300 cm^{-1}. The samples were evacuated at the following temperatures: (1) r.t., (2) 373, (3) 473, (4) 573, (5) 673 and (6) 873 K.

$g_{\|}$ = 2.36 value were indicative of an aqua complex. In addition, in the case of CuMFI(P)-100-75, the intensity of the $g_{\|}$ = 2.34-component band is considerably weaker than that of the $g_{\|}$ = 2.26-component band. On the basis of the fact that the intensity of the band due to the $[CuC_2H_5COO]^+$ species is weaker than that of the band due to $[CuOH]^+$,[16] the Cu^{2+} ions giving the $g_{\|}$ = 2.34 and 2.26 component bands were assigned to the $[CuC_2H_5COO]^+$ and $[CuOH]^+$ species, respectively.

The change in the state of copper ions in CuMFI by heat treatment *in vacuo* was elucidated. Fig. 8 shows the IR spectra obtained for CuMFI(P)-11.9-68 and CuMFI(P)-100-75 after evacuation at various temperatures. For CuMFI(P)-11.9-68 evacuated at 373 K, the intensity of the band at approximately 1650 cm^{-1} is considerably smaller than that for the r.t.-treated sample, indicating that the physisorbed water molecules were almost desorbed from the sample. In contrast, in the case of the 373 K-treated CuMFI(P)-100-75 sample, the 1650 cm^{-1}-band is slightly less intense. This result is due to the difference in the state of exchanged Cu^{2+}. The IR band in the range of 1700 to 1300 cm^{-1}, which is ascribed to the $[CuC_2H_5COO]^+$ species, disappears after evacuation at 573 K, thus indicating the decomposition of the propionate ion coordinated to Cu^{2+}.

Fig. 9 shows the EPR spectra for CuMFI(P)-11.9-68 and CuMFI(P)-100-75 evacuated at various temperatures. For the 373 K-treated CuMFI(P)-11.9-68 sample, two parameters were evaluated, indicating the existence of two kinds of exchangeable sites occupied by copper ions. The intensities of the observed bands decrease gradually with increases in the treatment temperature (*i.e.*, the reduction of Cu^{2+} to Cu^+).[38,40–42] No the values of two $g_{\|}$ parameters of CuMFI(P)-11.9-68 evacuated at above 473 K change, suggesting that these signals are due to the Cu^{2+} ions coordinated to lattice oxygen atoms. As regards CuMFI(P)-100-75 evacuated at temperatures of up to 473 K, the relevant parameters were identical to those for the r.t.-treated sample; the ligand fields around the Cu^{2+} ions hardly change. The state of the Cu^{2+} ions in the sample was negligibly affected by the desorption of physisorbed water molecules, as was also indicated by the result of the IR spectra (Fig. 8). Thus, from the results of Fig. 3, Fig. 6 and Fig. 7, we assigned the Cu^{2+} ions in CuMFI(P)-11.9-68 yielding $g_{\|}$ = 2.32 and $g_{\|}$ = 2.27 to the Cu^{2+} ions located in the neighbourhood of the three and the two lattice oxygen atoms, respectively. Evacuation of CuMFI(P)-100-75

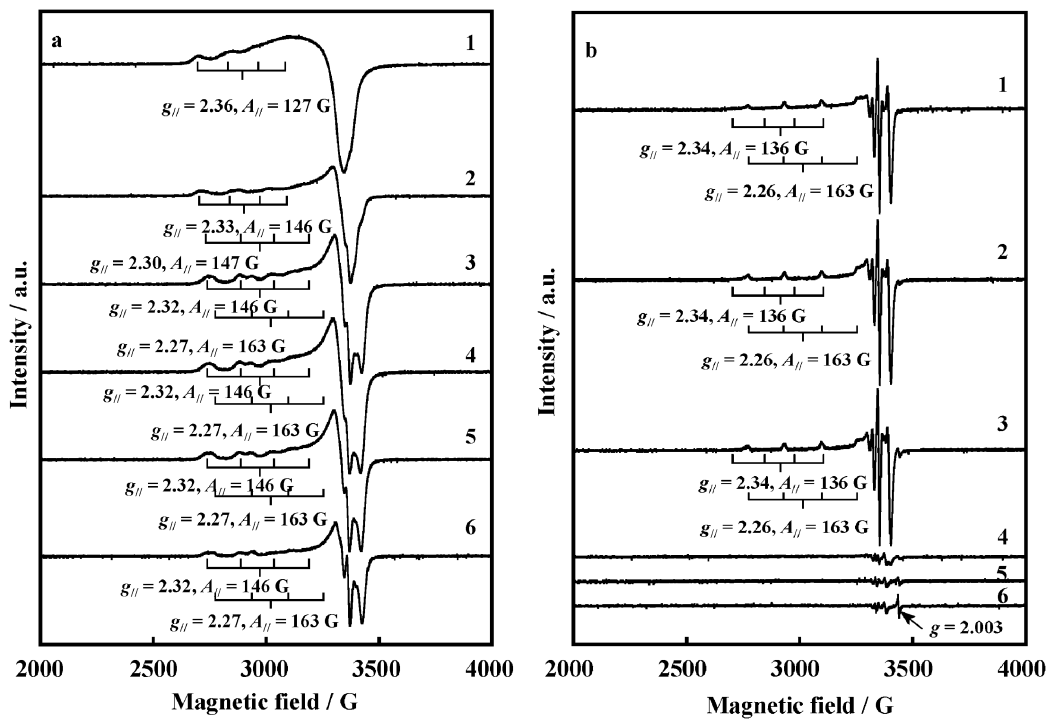

Fig. 9 EPR spectra of (a) CuMFI(P)-11.9-68 and (b) CuMFI(P)-100-75. The samples were evacuated at the following temperatures: (1) r.t., (2) 373, (3) 473, (4) 573, (5) 673 and (6) 873 K.

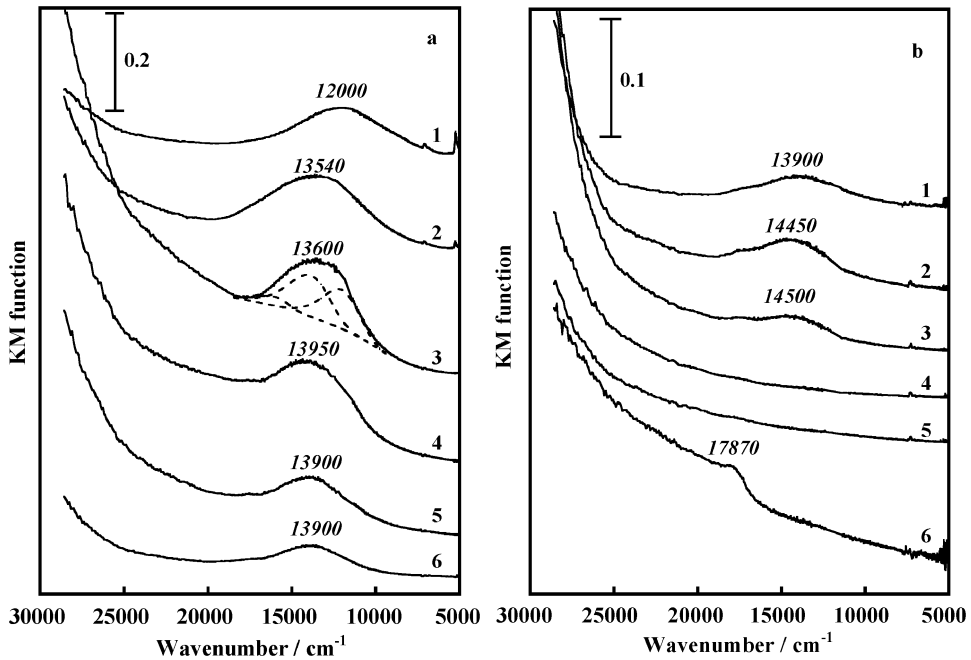

Fig. 10 DR-UV-Vis spectra of (a) CuMFI(P)-11.9-68 and (b) CuMFI(P)-100-75. The samples were evacuated at the following temperatures: (1) r.t., (2) 373, (3) 473, (4) 573, (5) 673 and (6) 873 K.

at 573 K led to a dramatic decrease in the intensity of the band. The reduction of the Cu^{2+} ions coordinated with the propionate ion to Cu^{+} appears to occur by evacuation at this temperature. In addition, in the case of CuMFI(P)-100-75 evacuated at 873 K, a sharp band is clearly seen in the vicinity of 3500 G ($g = 2.003$; this value was almost the same as that of the free electron ($g = 2.0023$)[43]), whereas this band is not seen in the case of CuMFI(P)-11.9-68.

The DR-UV-Vis spectra of CuMFI(P)-11.9-68 and CuMFI(P)-100-75 evacuated at various temperatures are represented in Fig. 10. For the 373 K-treated CuMFI(P)-11.9-68 sample, the position of the absorption maximum of the band due to the Cu^{2+} ions is shifted toward the side with the higher wavenumber, that is, by 1540 cm^{-1}, as compared to the position of the maximum for the r.t.-treated sample. This shift is due to the increased ligand-field strength caused by the stronger interaction between the Cu^{2+} ions and the oxygen atoms in the zeolite framework, which had been induced by the desorption of water molecules from the sample. In the case of CuMFI(P)-100-75, the extent of this shift is less marked (550 cm^{-1}). For other samples of CuMFI(P)-11.9-12, CuMFI(P)-19.8-72 and CuMFI(P)-35.0-50, the extent of the shift was 1520, 1250 and 870 cm^{-1}, respectively. For the band shift of CuMFI(C)-11.9-74 and CuMFI(C)-100-90, its extent was found to be, respectively 1540 and 1440 cm^{-1}. These results suggest that the relationship between the Si/Al ratio and the extent of the band shift strongly depended on the state of exchanged Cu^{2+} ions. The observed band for CuMFI(P)-11.9-68 evacuated at 473 K appears to involve at least three kinds of component bands: the bands centred at 16 500, 13 900 and 12 000 cm^{-1}. Taking account of the results described above (Fig. 6, Fig. 7 and Fig. 9) and our recent work,[44] the bands centred at 16 500 and 13 900 cm^{-1} could be ascribed to the Cu^{2+} ions located in the neighbourhood of the two and the three lattice oxygen atoms, respectively. For CuMFI(P)-11.9-68 evacuated at higher temperatures, the intensity of the band decreases gradually, which suggests a reduction of Cu^{2+} to Cu^{+}.[34,38] The 13 900 cm^{-1}-band observed for the r.t.-treated CuMFI(P)-100-75 sample disappears with evacuation at 573 K, although in the case of CuMFI(P)-11.9-68, the band due to the Cu^{2+} ions remains intact, even after evacuation at 873 K. For CuMFI(P)-100-75, the treatment temperature, 573 K, was the same temperature at which the band ascribed to the propionate ion coordinated to Cu^{2+} had disappeared (Fig. 8(b)). The results obtained for CuMFI(P)-19.8-72 and CuMFI(P)-35.0-50 were similar to those obtained for CuMFI(P)-100-75. Therefore, the extent of reduction clearly differed in a manner dependent on the Si/Al ratio of the samples, supporting the adsorption data. Noteworthy is that in the case of CuMFI(P)-100-75, a new band appears at 17 870 cm^{-1} with evacuation at 873 K. This band has been assigned to the plasmon resonance of metallic copper particles formed in the sample during heat treatment *in vacuo*.[45] On the basis of the observation that no such band was observed in the cases of CuMFI(C)-100-90, CuMFI(N)-100-73 and CuMFI(A) with various Si/Al ratios, the formation of metallic copper particles is assumed to be unique in the case of the sample with a higher Si/Al ratio when exposed to an aqueous solution of $Cu(C_2H_5COO)_2$.

Fig. 11 represents the TPD profiles for CuMFI(P)-11.9-68 and CuMFI(P)-100-75. For both samples, a desorption peak at around 373 K is derived from the desorption of physisorbed water in zeolite nanopores. In particular, in the case of CuMFI(P)-100-75, other distinct peaks are observed at 555, 660 and 715 K, which are, respectively ascribed to the desorption of CO_2, C_2H_4 and H_2, as a result of the decomposition of the propionate ion coordinated to the Cu^{2+} ions. These results clearly demonstrate the Si/Al ratio-dependent

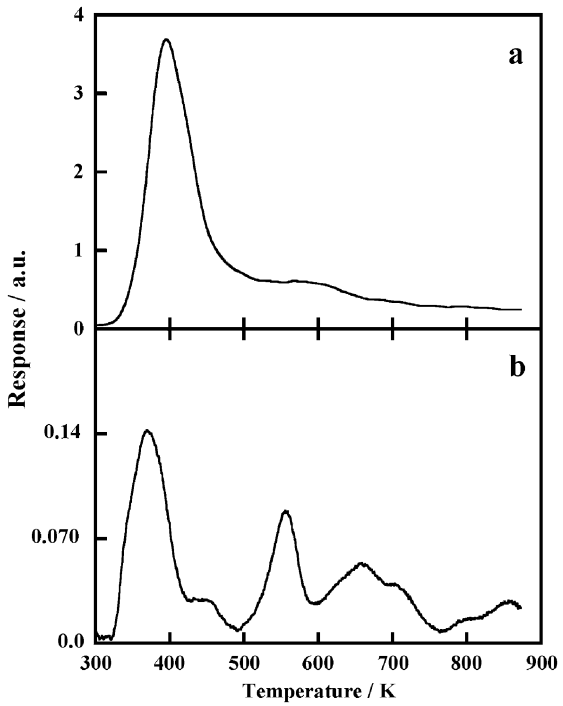

Fig. 11 TPD profiles for (a) CuMFI(P)-11.9-68 and (b) CuMFI(P)-100-75.

differences between species (molecules) desorbed from CuMFI during heat treatment. This difference undoubtedly originates from the different states of copper ions in the samples after ion exchange. In addition, it can be assumed that H_2 molecules, which are decomposition products of propionate ions, contribute to the reduction of Cu^+ to metallic copper in CuMFI(P) with higher Si/Al ratios.

More recently, interesting report has been made by Christensen's group; CuMEL and CuMTW exhibit efficient catalytic activity for the direct decomposition of NO, in comparison with CuMFI.[46] The difference in the catalytic activity was concluded to be caused by the difference in the location of active sites in samples. We here reported that by the difference in the Si/Al ratio of the mother MFI, the relative proportion of the number of the active sites in CuMFI for N_2 adsorption was considerably different. Referring to the model of the ion-exchange sites in MFI proposed by Nachtigallová *et al.*,[47] the two- and the three-coordinate sites presented are considered to correspond to I2 and M7 sites locating on the intersection of the straight and sinusoidal channels and on the main channel of MFI framework, respectively; the number of I2 sites were suggested to decrease with increasing the Si/Al ratio. Thus, the work of Christensen's group seems to have close connection with ours.

Conclusions

As regards N_2 adsorption at 301 K, CuMFI (Si/Al = 19.8) prepared by using a $Cu(C_2H_5COO)_2$ solution exhibited extremely efficient properties, as compared to the adsorption properties of samples with other Si/Al ratios and/or with other solutions. Furthermore, the three-coordinated Cu^+ species clearly exhibited effective for N_2 adsorption at r.t. and these species interact with N_2 molecules at a ratio of 1 : 1. The Cu^+ ions that exhibited a photoemission band at 18 500 cm^{-1} and gave a CO adsorption heat of 110 kJ mol^{-1} were formed in higher rate in samples with higher Si/Al ratios. This type of Cu^+ species had a three-coordinate structure involving lattice oxygen atoms. Taking account of the results of IR, DR-UV-Vis and EPR spectra for the r.t.-treated samples, it was concluded that Cu^{2+} ions with a propionate or acetate ion were exchanged in the neighbourhood of the three-coordinate sites.

Two different types of Cu^{2+} species in the two- and the three-coordinate sites were distinguishable by DR-UV-Vis and EPR spectral measurements. That is, the Cu^{2+} ions in the two-coordinate sites exhibit the DR-UV-Vis band at 16 500 cm^{-1} and the $g_{\|}$ = 2.27 parameter and the ones in the three-coordinate sites the DR-UV-Vis band at 13 900 cm^{-1} and the $g_{\|}$ = 2.32 parameter. Changes in the state of the copper ions in CuMFI induced by heat treatment *in vacuo* clearly differed in a manner dependent on the Si/Al ratios of the MFI. Metallic copper particles were formed in sample prepared by $Cu(C_2H_5COO)_2$ solution which had an Si/Al ratio of 100.

Experimental

Sodium-form MFI zeolite (NaMFI) with an Si/Al ratio of 11.9 and three types of protonic-form MFI zeolite (HMFI) with respective Si/Al ratios of 19.8, 35.0 and 100 (all supplied by Tosoh Co.) were used as the starting materials for the copper ion-exchange procedure. Approximately 5 g of MFI was dispersed in an aqueous solution of $Cu(C_2H_5COO)_2$ (pH 6.0), $Cu(CH_3COO)_2$ (pH 5.5), $CuCl_2$ (pH 3.0) or $Cu(NO_3)_2$ (pH 3.3) while being stirring for 1 h at a definite temperature. By repeating this operation several times, CuMFI samples with different Si/Al ratios and desired exchange levels were prepared. These samples were washed thoroughly with distilled water, followed by drying at room temperature (r.t.) in a vacuum desiccator for 24 h. The copper ion-exchange levels of the samples were determined according to the same method as that used previously.[3] The present samples are denoted as CuMFI(*X*)-*Y*-*Z* (*X*: type of counter ion employed, *i.e.*, P, A, C and N; *Y*: Si/Al ratio; *Z*: ion-exchange level). Detailed ion-exchange conditions and the resultant samples are described in the ESI.† N_2 gas, used as an adsorbate, was obtained by vaporizing liquid N_2. CO gas (99.9%) was purchased from the GL Sciences Co.

For the sample treated at 873 K for 4 h under a reduced pressure of 1 mPa, the adsorption isotherms of N_2 or CO were obtained volumetrically at 301 K. The heat of adsorption was measured simultaneously with the adsorption isotherms by using an adiabatic-type calorimeter.[48]

The photoemission spectra were measured at r.t. with a Hitachi F-2000 photoluminescence spectrophotometer. The emission was observed by focusing an excitation light of 33 300 cm^{-1} onto an *in situ* sample cell.

The X-ray absorption fine structure (XAFS) spectra were taken at beam line 10B, which was equipped with a double-crystal monochrometer of Si(311), under ring-operating

conditions of 2.5 GeV and 300 mA (Photon Factory in the Institute of Materials Structure Science: Inter-university Research Institute Corporation, High Energy Accelerator Research Organization, KEK, Tsukuba). The photon energy was calibrated by using the pre-edge peak of a copper foil (8.9788 keV). The X-ray absorption near edge structure (XANES) and the extended X-ray absorption fine structure (EXAFS) spectra were recorded at energy intervals of 0.5 eV and 2–3 eV, respectively. A self-supporting disk was loaded into an *in situ* cell. The spectral data were analysed using Maeda's program.[49]

For the measurement of infrared (IR) spectra, a self-supporting sample disk was loaded into an IR cell. The spectra were recorded at r.t. on a Digilab FTS4000MXK FT-IR spectrophotometer equipped with a TGS detector (accumulation: 64 scans; resolution: 4 cm^{-1}). The intensity of the IR band was corrected by normalizing the intensity of the skeletal mode of zeolite at approximately 2000 cm^{-1}.

The diffuse reflectance UV-Vis (DR-UV-Vis) spectral data were collected at r.t. using a JASCO 550 UV-Vis spectrophotometer equipped with an integrating-sphere attachment. The sample was placed into a vacuum reflectance cell. Spectralon (Labsphere, USA) was employed as a reference material.

The electron paramagnetic resonance (EPR) spectra were recorded at r.t. with a JEOL-FE3XG spectrometer operating at about 9.5 GHz. The measurements were carried out under the following conditions: field modulation, 100 kHz; microwave power, 1 mW; and modulation width, 5 Gauss. The sample was loaded into an EPR sample tube equipped with a stop cock. The resonance magnetic field was determined by using a manganese species doped into the solid material as a reference.

Prior to measurements of the spectra, each sample was treated at a definite temperature for 2 h under a reduced pressure of 1 mPa.

The temperature-programmed desorption (TPD) profiles were obtained by using an apparatus equipped with a thermal conductivity detector (GL Sciences, Type E-12). The sample was treated at r.t. for 2 h under a reduced pressure of 1 mPa before the thermal desorption run, and then the sample was heated to 873 K at a rate of 5 K min^{-1} under flowing He gas at a rate of 60 cm^3 min^{-1}. Desorbed gases were monitored by an ANELVA M-100QA-F mass spectrometer.

Acknowledgements

This work was supported by Grant-in-Aid for Scientific Research (Nos. 15350082, 17034046, 17655061 and 17036043) from the Ministry of Education, Culture, Sports, Science and Technology of Japan. The measurement of XAFS spectra was carried out under the proposal (Nos. 2004G092 and 2004G329) of the Photon Factory Program Advisory Committee. We thank Drs M. Nomura, Y. Inada and A. Koyama of KEK in Tsukuba for their kind assistance in measuring the XAFS spectra. A. Itadani acknowledges the Research Fellowship from Okayama University.

References

1 (*a*) M. Iwamoto, H. Furukawa, Y. Mine, F. Uemura, S. Mikuriya and S. Kagawa, *J. Chem. Soc., Chem. Commun.*, 1986, 1272; (*b*) M. Iwamoto and H. Yahiro, *Catal. Today*, 1994, **22**, 5.
2 M. Shelef, *Chem. Rev.*, 1995, **95**, 209.
3 (*a*) Y. Kuroda, S. Konno, K. Morimoto and Y. Yoshikawa, *J. Chem. Soc., Chem. Commun.*, 1993, 18; (*b*) Y. Kuroda, Y. Yoshikawa, S. Konno, H. Hamano, H. Maeda, R. Kumashiro and M. Nagao, *J. Phys. Chem.*, 1995, **99**, 10621; (*c*) Y. Kuroda, Y. Yoshikawa, S. Emura, R. Kumashiro and M. Nagao, *J. Phys. Chem. B*, 1999, **103**, 2155.
4 G. Spoto, S. Bordiga, G. Ricchiardi, D. Scarano, A. Zecchina and F. Geobaldo, *J. Chem. Soc., Faraday Trans.*, 1995, **91**, 3285.
5 S. Recchia, C. Dossi, R. Psaro, A. Fusi, R. Ugo and G. Moretti, *J. Phys. Chem. B*, 2002, **106**, 13326.
6 E. Giamello, D. Murphy, G. Magnacca, C. Morterra, Y. Shioya, T. Nomura and M. Anpo, *J. Catal.*, 1992, **136**, 510.
7 J. Dědeček, Z. Sobalík, Z. Tvarůžková, D. Kaucký and B. Wichterlová, *J. Phys. Chem.*, 1995, **99**, 16327.
8 C. Lamberti, S. Bordiga, M. Salvalaggio, G. Spoto, A. Zecchina, F. Geobaldo, G. Vlaic and M. Bellatreccia, *J. Phys. Chem. B*, 1997, **101**, 344.
9 Y. Kuroda, Y. Yoshikawa, R. Kumashiro and M. Nagao, *J. Phys. Chem. B*, 1997, **101**, 6497.
10 P. Nachtigall, D. Nachtigallová and J. Sauer, *J. Phys. Chem. B*, 2000, **104**, 1738.
11 (*a*) Y. Kuroda, R. Kumashiro, T. Yoshimoto and M. Nagao, *Phys. Chem. Chem. Phys.*, 1999, **1**, 649; (*b*) Y. Kuroda, K. Yagi, N. Horiguchi, Y. Yoshikawa, R. Kumashiro and M. Nagao, *Phys. Chem. Chem. Phys.*, 2003, **5**, 3318.
12 Y. Kuroda and M. Iwamoto, *Top. Catal.*, 2004, **28**, 111.
13 A. Itadani, Y. Kuroda, M. Tanaka and M. Nagao, *Microporous Mesoporous Mater.*, 2005, **86**, 159.
14 Y. Kuroda, R. Kumashiro, A. Itadani, M. Nagao and H. Kobayashi, *Phys. Chem. Chem. Phys.*, 2001, **3**, 1383.
15 A. Itadani, R. Kumashiro, Y. Kuroda and M. Nagao, *Thermochim. Acta*, 2004, **416**, 99.
16 A. Itadani, Y. Kuroda and M. Nagao, *Microporous Mesoporous Mater.*, 2004, **70**, 119.
17 Y. Kuroda, A. Itadani, R. Kumashiro, T. Fujimoto and M. Nagao, *Phys. Chem. Chem. Phys.*, 2004, **6**, 2534.
18 For example: D. W. Breck, *Zeolite Molecular Sieves*, John Wiley, New York, 1984.
19 For example: (*a*) Y. Li and W. K. Hall, *J. Catal.*, 1991, **129**, 202; (*b*) G. Moretti, *Catal. Lett.*, 1994, **23**, 135; (*c*) C. Torre-Abreu, M. F. Ribeiro, C. Henriques and F. R. Ribeiro, *Appl. Catal., B*, 1997, **11**, 383; (*d*) C. Torre-Abreu, M. F. Ribeiro, C. Henriques and G. Delahay, *Appl. Catal., B*, 1997, **12**, 249; (*e*) B. Wichterlová, J. Dědeček, Z. Sobalík, A. Vondrová and K. Klier, *J. Catal.*, 1997, **169**, 194.
20 Y. Kuroda, T. Okamoto, R. Kumashiro, Y. Yoshikawa and M. Nagao, *Chem. Commun.*, 2002, 1758.
21 M. Iwamoto and Y. Hoshino, *Inorg. Chem.*, 1996, **35**, 6918.
22 K. I. Hadjiivanov, M. M. Kantcheva and D. J. Klissurski, *J. Chem. Soc., Faraday Trans.*, 1996, **92**, 4595.
23 R. Bulánek, B. Wichterlová, Z. Sobalík and J. Tichý, *Appl. Catal., B*, 2001, **31**, 13.
24 (*a*) R. Bulánek, P. Čičmanec, P. Knotek, D. Nachtigallová and P. Nachtigall, *Phys. Chem. Chem. Phys.*, 2004, **6**, 2003; (*b*) R. Bulánek, *Phys. Chem. Chem. Phys.*, 2004, **6**, 4208.
25 R. Bulánek, H. Drobná, P. Nachtigall, M. Rubeš and O. Bludský, *Phys. Chem. Chem. Phys.*, 2006, **8**, 5535.
26 M. Davidová, D. Nachtigallová, R. Bulánek and P. Nachtigall, *J. Phys. Chem. B*, 2003, **107**, 2327.
27 O. Bludský, P. Nachtigall, P. Čičmanec, P. Knotek and R. Bulánek, *Catal. Today*, 2005, **100**, 385.
28 Y. Kuroda, T. Mori, Y. Yoshikawa, S. Kittaka, R. Kumashiro and M. Nagao, *Phys. Chem. Chem. Phys.*, 1999, **1**, 3807.
29 L.-S. Kau, D. J. Spira-Solomon, J. E. Penner-Hahn, K. O. Hodgson and E. I. Solomon, *J. Am. Chem. Soc.*, 1987, **109**, 6433.
30 L.-S. Kau, K. O. Hodgson and E. I. Solomon, *J. Am. Chem. Soc.*, 1989, **111**, 7103.
31 A. Zecchina, F. Geobaldo, G. Spoto, S. Bordiga, G. Ricchiardi, R. Buzzoni and G. Petrini, *J. Phys. Chem.*, 1996, **100**, 16584.

32 A. Jentys, G. Warecka, M. Derewinski and J. A. Lercher, *J. Phys. Chem.*, 1989, **93**, 4837.
33 G. B. Deacon and R. J. Phillips, *Coord. Chem. Rev.*, 1980, **33**, 227.
34 J. Texter, D. H. Strome, R. G. Herman and K. Klier, *J. Phys. Chem.*, 1977, **81**, 333.
35 (*a*) Y. Teraoka, C. Tai, H. Furukawa, S. Kagawa, K. Asakura and Y. Iwasawa, *Shokubai*, 1990, **32**, 426; (*b*) Y. Teraoka, C. Tai, H. Ogawa, H. Furukawa and S. Kagawa, *Appl. Catal., A*, 2000, **200**, 167.
36 R. A. Schoonheydt, *Catal. Rev. Sci. Eng.*, 1993, **35**, 129.
37 M. L. Jacono, G. Fierro, R. Dragone, X. Feng, J. d'Itri and W. K. Hall, *J. Phys. Chem. B*, 1997, **101**, 1979.
38 G. T. Palomino, P. Fisicaro, S. Bordiga, A. Zecchina, E. Giamello and C. Lamberti, *J. Phys. Chem. B*, 2000, **104**, 4064.
39 C.-C. Chao and J. H. Lunsford, *J. Chem. Phys.*, 1972, **57**, 2890.
40 M. W. Anderson and L. Kevan, *J. Phys. Chem.*, 1987, **91**, 4174.
41 S. C. Larsen, A. Aylor, A. T. Bell and J. A. Reimer, *J. Phys. Chem.*, 1994, **98**, 11533.
42 A. V. Kucherov, H. G. Karge and R. Schlögl, *Microporous Mesoporous Mater.*, 1998, **25**, 7.
43 R. J. Myers, *Molecular Magnetism and Magnetic Resonance Spectroscopy*, Prentice-Hall, Englewood Cliffs, NJ, 1973.
44 A. Itadani, M. Tanaka, T. Mori, M. Nagao, H. Kobayashi and Y. Kuroda, *J. Phys. Chem. C*, in press.
45 H. Wang, F. Tam, N. K. Grady and N. J. Halas, *J. Phys. Chem. B*, 2005, **109**, 18218.
46 (*a*) M. Yu. Kustova, A. Kustov, S. E. Christiansen, K. T. Leth, S. B. Rasmussen and C. H. Christensen, *Catal. Commun.*, 2006, **7**, 705; (*b*) M. Yu. Kustova, S. B. Rasmussen, A. L. Kustov and C. H. Christensen, *Appl. Catal., B*, 2006, **67**, 60.
47 D. Nachtigallová, P. Nachtigall, M. Sierka and J. Sauer, *Phys. Chem. Chem. Phys.*, 1999, **1**, 2019.
48 T. Matsuda, H. Taguchi and M. Nagao, *J. Therm. Anal.*, 1992, **38**, 1835.
49 H. Maeda, *J. Phys. Soc. Jpn.*, 1987, **56**, 2777.

